

This preprint has been accepted for publication in *Journal of Hydrology*. The published version is available at <https://doi.org/10.1016/j.jhydrol.2025.134686>.

**Trade-offs Between Discretization Approaches in Urban Stormwater Modeling: Accuracy, Interpretability, and Practical Implications**

Zhaokai Dong<sup>a\*</sup>, Sabrina Jivani<sup>a</sup>, Pradeep Goel<sup>b</sup>, and Clare E. Robinson<sup>a</sup>

<sup>a</sup> Department of Civil and Environmental Engineering, Spencer Engineering Building, Western University, 1151 Richmond St, London, ON N6A 3K7, Canada.

<sup>b</sup> Water Monitoring Section, Environmental Monitoring and Reporting Branch, Ministry of the Environment, Conservation and Parks, 125 Resources Road Etobicoke, ON, M9P3V6, Canada.

\*Corresponding author email: [zdong262@uwo.ca](mailto:zdong262@uwo.ca)

1    **Abstract**

2    Stormwater models are important tools for urban drainage design, planning, and analysis, but  
3    their performance and interpretation depend heavily on how spatial discretization is handled.  
4    This study evaluates the influence of two common discretization strategies – topography- and  
5    sewer geometry-based – on hydrological representation and simulation accuracy in the Storm  
6    Water Management Model (SWMM), using a mixed urban and peri-urban watershed in London,  
7    ON, Canada. Leveraging long-term flow data from multiple monitoring locations across the  
8    watershed, we systematically evaluated the effects of discretization strategy across different  
9    rainfall conditions and land use settings (e.g., urban vs. peri-urban) using continuous and event-  
10   based simulations, as well as a fixed-effects regression model. The two models with different  
11   discretization approaches showed no significant differences in simulating outlet flows (mean  
12    $NSE = 0.88$  for the topography-based model and 0.85 for the sewer geometry-based model).  
13   However, the topography-based model yielded parameter values with greater hydrological  
14   interpretability and, accordingly, performed better at simulating flows at locations within the  
15   watershed ( $NSE = 0.74$ –0.86) compared to the geometry-based model ( $NSE = 0.55$ –0.83). In  
16   addition, model performance was strongly influenced by rainfall depth and land use  
17   characteristics, with significantly improved results observed during larger storm events and in  
18   the urban watershed. Ultimately, the study demonstrates that discretization choice can  
19   significantly influence model structure, parameter interpretation, and spatial simulation accuracy.  
20   While the topography-based approach enhances hydrological representation, the sewer  
21   geometry-based model remains a practical and efficient alternative particularly in data-limited  
22   areas.

23    **Keywords**

24    Stormwater modeling; discretization; hydrological representation; SWMM; spatial data  
25    processing; urban and peri-urban watersheds

26 **1. Introduction**

27 Urban stormwater management is a major challenge as urbanization increases impervious  
28 surface cover, resulting in higher stormwater flow volumes and peak flow rates (Hopkins et al.,  
29 2014, Jefferson et al., 2017). To support stormwater regulation and planning, hydrologic-  
30 hydraulic stormwater models – such as the U.S. EPA Storm Water Management Model  
31 (SWMM) – are widely used to simulate flow responses of urban drainage systems to  
32 precipitation events (Niazi et al., 2017). These models help planners and practitioners assess  
33 existing drainage infrastructure networks, evaluate and design stormwater control measures, and  
34 evaluate alternative land use scenarios (Tamm et al., 2023 Javan et al., 2025 Khatooni et al.,  
35 2025).

36 Spatial discretization of the watershed is an essential step in constructing stormwater models  
37 whereby the boundaries of subcatchments (fundamental drainage areas) that direct local runoff to  
38 sewer systems are determined (Rossman and Huber, 2016). In urban settings, this task is  
39 challenging as runoff pathways are influenced by both the engineered drainage infrastructure  
40 (e.g., sewer inlets and pipes) and complex human-modified surface topography (Gironás et al.,  
41 2010, Dong et al., 2022). At high spatial resolution, small urban parcels (e.g., buildings) can be  
42 modeled as individual subcatchments, routing overland flow to a nearby sewer inlet, which  
43 closely reflects actual drainage behavior. While effective at the block scale, such fine-scale  
44 mapping is time-intensive and often not practical for larger watersheds or scenario-based  
45 planning (Dong et al., 2022, Si et al., 2024). Hence, model discretization approaches that can  
46 provide physically based representation of stormwater drainage behavior but with reduced spatial  
47 complexity are favored for larger-scale models (greater than a few blocks) (Dobson et al., 2022).

48 Two simplification strategies are commonly used for discretization of large watersheds. The first  
49 is a topography-based approach, which uses digital elevation models (DEMs) to determine  
50 subcatchment boundaries and outlets. Since drainage infrastructure is not represented in DEMs,  
51 sewer network data is often integrated with the subcatchment delineation to manually define  
52 surface-subsurface flow paths (i.e., connecting subcatchment outlets to sewer inlets) (Si et al.,  
53 2024). To improve efficiency, “burning” techniques have also been used to improve  
54 representation of engineered drainage pathways by lowering DEM elevations along known sewer  
55 alignments such as sewer inlets or pipes (Gironás et al., 2010 Sokolovskaya et al., 2023 Si et al.,  
56 2024). However, discretization outcomes (e.g., drainage boundaries) are sensitive to the quality  
57 and resolution of DEM data (Leitão et al., 2009, Salvadore et al., 2015). For example,  
58 Sokolovskaya et al. (2023) found that DEMs, with a resolution coarser than approximately 1.5  
59 m, may not be able to capture relevant urban microtopographic features as needed to derive  
60 realistic drainage areas. Similarly, Zhou et al. (2021) highlighted that a fine-resolution DEM  
61 (~0.2 m) is necessary to delineate reliable drainage areas in flat urban terrains. Despite the  
62 increasing availability of freely available high-resolution DEMs (e.g., LiDAR-derived datasets),  
63 their spatial coverage remains patchy across cities, particularly in developing regions. As a  
64 result, modelers continue to rely on coarser global DEM products (e.g., SRTM) in many areas,  
65 which can hinder accurate delineation of drainage boundaries (Hawker et al., 2019).

66 The second strategy is a sewer geometry-based approach, where watersheds are discretized by  
67 drawing Thiessen polygons around the sewer inlets. This method directs surface runoff within  
68 each polygon to its nearest inlet, thereby simplifying the physical definition of drainage  
69 boundaries and their connection to the sewer system. Recently, the sewer geometry-based  
70 approach has gained popularity due to its ease of use and efficient integration with available

71 infrastructure datasets (Dong et al., 2022, Li et al., 2024, Ni et al., 2025, Qi et al., 2025).  
72 However, the lack of consideration for topographic characteristics may result in less accurate  
73 representation of terrain-driven flow patterns, such as runoff along roads to drains. This  
74 limitation may reduce the accuracy of the model in simulating flow accumulation within the  
75 watershed, potentially leading to misclassification of areas vulnerable to localized flooding.

76 Despite their distinct strengths and limitations, the topography-based (e.g., Warsta et al., 2017,  
77 Swathi et al., 2019) and geometry-based (e.g., Dong et al., 2022, Li et al., 2024) discretization  
78 approaches have both been successfully applied to develop stormwater models. Yet, the  
79 performance of these models has largely been evaluated using data collected from single  
80 monitoring locations, often at the watershed outlet. As a result, it remains unclear whether  
81 alternative discretization approaches lead to differences in the representation of hydrological  
82 processes within a watershed, such as subcatchment-scale parameter estimates and simulated  
83 flows. More specifically, it is unknown whether the increased complexity of topography-based  
84 discretization improves flow simulations within the watershed compared to the simpler  
85 geometry-based discretization approach. This question is particularly important in urban areas  
86 where calibration and validation are often constrained by limited rainfall-flow data, typically  
87 available only at the watershed outlet (Broekhuizen et al., 2020). A few studies have  
88 qualitatively compared the two discretization approaches. For example, Li et al. (2024) recently  
89 conducted scenario-based simulations to compare node surcharge responses from models  
90 developed using the two discretization approaches. They reported comparable total overflow  
91 volumes between the two models (absolute difference < 5%), although discrepancies increased  
92 with increasing storm magnitudes. Dong et al. (2022) compared flow simulations between  
93 topography- and geometry-based models at the outlet of a small urban watershed and found that

94 the two models produced comparable peak flows relative to observations. However, the analyses  
95 of Li et al. (2024) and Dong et al. (2022) were limited to scenario-based or uncalibrated  
96 simulations and neither study examined how the discretization approach influences parameter  
97 calibration, flow simulations within the watershed, or the consistency of model performance  
98 across different storm events.

99 In urban-rural transitional (peri-urban) areas, natural drainage and engineered stormwater  
100 infrastructure (e.g., sewer systems) both exist (Niazi et al., 2017), often resulting in a  
101 combination of fast and slow hydrological responses to storm events (Braud et al., 2013). In such  
102 settings, different discretization methods may yield distinct representations of dominant drainage  
103 processes, given their different underlying assumptions (i.e., topography-driven versus sewer-  
104 network-driven), potentially making one approach more suitable than another depending on the  
105 degree of urbanization and drainage characteristics. With urban areas rapidly expanding  
106 worldwide, understanding how spatial discretization choices influence model performance across  
107 watersheds with varying land use and drainage configurations is important for developing robust  
108 stormwater models that balance complexity and applicability for planning and design purposes.  
109 To fill these gaps, this study systematically evaluates the influence of discretization approach on  
110 model structure, parameter interpretation, and performance under varying rainfall and land use  
111 conditions.

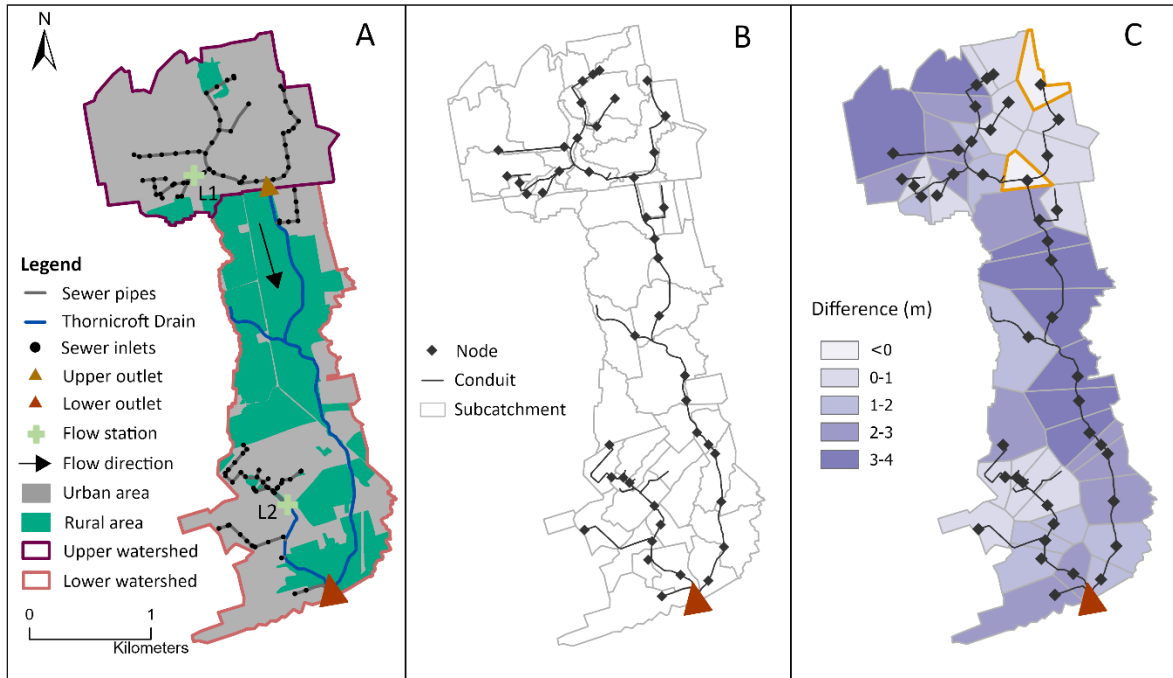
112 The objective of this study is to evaluate and compare the performance, sensitivity, and  
113 interpretability of stormwater models developed using topography- and sewer geometry-based  
114 discretization approaches. To address this, we develop two SWMM models of a highly  
115 monitored watershed in London, Canada using topography-based and sewer geometry-based

116 discretization approaches. Using continuous and event-based simulations, along with fixed-  
117 effects regression, we evaluate how discretization strategy affects model performance across  
118 different land use types, storm event sizes, and monitoring locations at the outlets and within the  
119 watershed. This quantitative comparison is used to clarify the tradeoffs in selecting a  
120 discretization strategy including model physical realism, simplicity of implementation, and  
121 model performance. Overall, this study provides new insights to support discretization strategy  
122 selection for efficient, reliable stormwater scenario simulations.

123 **2. Methods**

124 **2.1 Study site and data**

125 The study area is the Thornicroft Drain watershed, located in London, ON, Canada (Figure 1A  
126 and Figure S1 Supplementary Material (SM)). The watershed area is approximately 580 ha. The  
127 upper watershed (~210 ha) is highly urbanized, with 94% of the area consisting of urban land  
128 uses, including residential, commercial, industrial, and transportation. Runoff is collected and  
129 conveyed through a separated sewer system and discharged to the Thornicroft Drain open  
130 channel at the upper outlet. The lower watershed (~370 ha) is a peri-urban area comprising 50%  
131 rural land uses, including agricultural land and forest. Most runoff in the lower watershed drains  
132 directly to the Thornicroft Drain, except for one residential neighborhood (~100 ha) that is  
133 serviced by a separated sewer system that ultimately discharges into the Thornicroft Drain. The  
134 primary soil type in urban land use areas is silty clay, while silty sand is the primary soil type in  
135 rural land use areas. Hereafter, we refer to the upper watershed as the upper urban watershed and  
136 the lower watershed as the lower peri-urban watershed, based on their distinct land use  
137 characteristics and stormwater drainage infrastructure.



139 **Figure 1.** (A) major land use within upper watershed and lower watershed areas, stormwater  
 140 drainage pathways, and flow monitoring stations at the outlets of the upper and lower watersheds  
 141 and at two locations within the watershed (L1 and L2). Model configurations developed based on  
 142 (B) topography-based discretization and (C) sewer geometry-based discretization. Elevation  
 143 difference between subcatchment average elevation and corresponding node elevation for sewer  
 144 geometry-based discretization model is shown in panel (C). Subcatchments for which the  
 145 average surface elevation is less than the node elevation are marked with orange border.

146 Stormwater flow monitoring was conducted from August 2021 to November 2023 at the outlets  
 147 of the upper urban watershed and the lower peri-urban watershed. At these locations water levels  
 148 in Thornicroft Drain were continuously measured at 15-minute intervals using a pressure  
 149 transducer (TD/CTD Diver, Van Essen Instruments). Measured water levels were converted to  
 150 flow rates by developing rating curves for each location. These rating curves were based on flow  
 151 rate measurements performed using a portable flow meter (HACH FH950) across a wide range

152 of flow conditions. Over the same monitoring period, flows were also measured at two locations  
153 within the watershed – L1 (a storm drain) within the upper urban watershed and L2 (an open  
154 drain) within the lower peri-urban watershed. These locations were selected because they are  
155 accessible for continuous flow monitoring and represent flows from distinct land uses within the  
156 upper (urban) and lower (peri-urban) portions of the watershed. However, even with regular site  
157 visits and equipment maintenance, sediment build-up and sewer backwater in these drains  
158 occasionally affected flow measurements. Therefore, flow data for some individual events  
159 needed to be excluded from the simulations. Further details of the monitoring program and  
160 dataset are available in Vyn (2023). As snowmelt data during the monitoring period are not  
161 available, this study focuses on simulating stormwater flows during the warm season (June to  
162 October).

163 Rainfall data with 5-minute resolution were obtained from two City of London rain gauges  
164 located 0.6 km southwest and 1.7 km northeast of the watershed boundary (Figure S1). Sewer  
165 infrastructure data, including spatial layout and pipe geometry, were provided by the City of  
166 London. Spatial datasets were obtained from the Ontario Ministry of Natural Resources and  
167 Forestry (OMNRF, 2019), including a 2-m LiDAR-derived digital elevation model (DEM) and  
168 0.5-m resolution aerial imagery. Daily climate data, including minimum and maximum  
169 temperatures, were collected from Environment and Climate Change Canada (EMCC, 2024). A  
170 summary of all datasets used in this study is provided in SM Table S1.

## 171 **2.2 Model development**

172 The U.S. EPA Storm Water Management Model (SWMM) was used to simulate stormwater  
173 flows in the study watershed. SWMM is a widely used for urban stormwater simulations

174 (Rossman and Huber, 2016). It simulates runoff generation from subcatchments (the basic  
175 hydrological units) and routes the resulting flow through sewer networks to an outfall. Watershed  
176 discretization, a fundamental step in model development, involves delineating subcatchment  
177 boundaries and specifying the direction of runoff toward sewer inlets. In this study, two SWMM  
178 models were developed using the same precipitation input and sewer data (Table S1), but with  
179 the watershed discretized using topography- and sewer geometry-based methods, respectively.

180 For the topography-based model, subcatchment boundaries were delineated using ArcGIS  
181 hydrologic analysis tools applied to raw DEM data. These included sink filling, flow direction  
182 and accumulation, and watershed basin delineation (Bibi, 2022). In urban areas, the resulting  
183 subcatchments were overlaid with sewer network data to refine boundaries and assign  
184 subcatchment outlets to sewer inlets. This task was completed with additional input from City of  
185 London municipal engineers to ensure that the assigned subcatchment-sewer connections were  
186 consistent with the actual drainage conditions, with adjustments made where discrepancies were  
187 identified. For subcatchments without nearby sewer infrastructure, runoff was routed to adjacent  
188 downstream subcatchments or directly to Thornicroft Drain.

189 In the sewer geometry-based model, watershed discretization was completed by drawing  
190 Thiessen polygons around nodes (e.g., sewer inlets), such that any point within a polygon is  
191 closer to its corresponding node than to any other node (i.e., representing the shortest flow path).  
192 This approach assumes that each node is located at a minimum local elevation, allowing runoff  
193 from the surrounding area to be routed to that node (Dong et al., 2022). Although Dong et al.  
194 (2022) showed that the location of nodes used to generate polygons does not significantly impact  
195 outlet flow simulations, identical node locations were used in both the topography-based and  
196 sewer geometry-based models to ensure consistent comparisons of inflows at each node.

197 Specifically, subcatchment outlets from the topography-based model were used to generate  
198 polygons.

199 The slope and imperviousness parameters for each subcatchment were first determined using  
200 DEM data and aerial imagery (Figure S2). As SWMM assumes spatial-uniform characteristics  
201 within each subcatchment, area-weighted averages were assigned to each subcatchment.  
202 Subcatchment width, representing the stormwater overland flow width, was inferred from spatial  
203 data. In the topography-based model, the subcatchment width was initially calculated by dividing  
204 the subcatchment area by the flow path length determined from the DEM, with outlets typically  
205 located at the downslope edge of the subcatchment (Figure S2A). In the sewer geometry-based  
206 model, subcatchment width was estimated by dividing the subcatchment area by a two-sided  
207 symmetrical flow length (Rossman and Huber, 2016). The one-side flow length (i.e., half of the  
208 two-sided symmetrical length) was calculated as the longest distance from any point within the  
209 subcatchment to its corresponding sewer inlet (Dong et al., 2022).

210 Other parameters were obtained from literature, including Manning's roughness, depression  
211 storage, and pipe roughness (Krebs et al., 2014 Bisht et al., 2016 Lee et al., 2018 Macro et al.,  
212 2019 Perin et al., 2020 Behrouz et al., 2020 Dong et al., 2022 Zhuang et al., 2023 Wu et al.,  
213 2024). In both models, infiltration was simulated using the Green-Ampt method, which requires  
214 specification of soil parameters including saturated hydraulic conductivity, suction head, and  
215 initial moisture deficit. This method was applied because it provides a physically based  
216 representation of infiltration processes, with parameters that can be approximated using literature  
217 values that are based on extensive measurements for different soil classes (Rossman and Huber,  
218 2016). Subsurface flow was simulated using the SWMM groundwater module, which represents  
219 surface runoff-groundwater interactions by simulating water movement between an upper

220 unsaturated soil zone and a lower saturated soil zone. Parameters estimated for this module  
221 include aquifer porosity, field capacity, and saturated hydraulic conductivity. Parameter values  
222 related to infiltration and groundwater modules were adopted from a previous study by Jivani  
223 (2024), who calibrated these parameters using flow data measured within the watershed. Further  
224 information on estimation of these parameters and values used is provided in Table S2.

225 **2.3 Model calibration and evaluation**

226 Model calibration was performed using continuous flow data from August to October 2021.  
227 Given the distinct land use characteristics between the upper and lower watersheds, the  
228 parameters for subcatchments in the upper urban watershed were first calibrated using the upper  
229 outlet flow data. Following this, the parameters for subcatchments in the lower peri-urban  
230 watershed were calibrated using lower outlet flow data, while keeping the parameters calibrated  
231 for the upper subcatchments fixed. This stepwise calibration helped reduce the influence of  
232 parameterization in the upper watershed on simulations in the lower watershed. A warm-up  
233 period of 15 days was used to stabilize initial conditions. Parameters for calibration included  
234 subcatchment width, Manning's roughness, depression storage, and pipe roughness. The Nash-  
235 Sutcliffe Efficiency (NSE, Equation 1) (Nash and Sutcliffe, 1970) was used as the primary  
236 performance evaluation metric (both for calibration and validation), with this metric  
237 supplemented by runoff volume error (Equation 2), peak flow error (Equation 3), and time-to-  
238 peak error (Equation 4), and flow residuals (Equation 5). Model calibration was conducted using  
239 Monte Carlo simulations (Dong et al., 2022), in which parameters were randomly sampled from  
240 the ranges provided in Table S2. For each model, 1,000 simulation runs were executed, and the  
241 parameter set from the best-performing run which yielded the highest NSE value was selected  
242 for validation.

243 
$$\text{NSE} = 1 - \frac{\sum_{i=1}^n (Q_{o,i} - Q_{s,i})^2}{\sum_{i=1}^n (Q_{o,i} - \bar{Q}_o)^2}$$
 Equation 1

244 
$$\text{Volume error} = \frac{\sum_{i=1}^n (Q_{o,i} - Q_{s,i})}{\sum_{i=1}^n (Q_{o,i})} \times 100\%$$
 Equation 2

245 
$$\text{Peak flow error} = \frac{(P_{o,i} - P_{s,i})}{P_{o,i}} \times 100\%$$
 Equation 3

246 Time-to-peak error =  $(t_{o,i} - t_{s,i})$  Equation 4

247 Flow residual =  $Q_{s,i} - Q_{o,i}$  Equation 5

248 where  $Q_{o,i}$  and  $Q_{s,i}$  are the observed and simulated flow rates ( $\text{m}^3/\text{s}$ ), respectively,  $\bar{Q}_o$  is the  
 249 observed mean flow ( $\text{m}^3/\text{s}$ );  $P_{o,i}$  and  $P_{s,i}$  are the observed and simulated peak flow rates ( $\text{m}^3/\text{s}$ ),  
 250 respectively, and  $t_{o,i}$  and  $t_{s,i}$  are the time corresponding to the observed and simulated peak flow  
 251 rates (min), respectively. An NSE value closer to 1 indicates better model performance.

252 Validation was conducted using continuous flow data from June to October for 2022 and 2023 at  
 253 the upper and lower watershed outlets, along with two monitoring locations that are within the  
 254 upper urban watershed (L1) and lower peri-urban watershed (L2), respectively (flow data from  
 255 2021-2023). In addition to calibrating and validating the model based on continuous flow  
 256 simulations, model performance was also evaluated at the event scale. To define individual storm  
 257 events, we tested dry inter-event periods of four hours (Alivio et al., 2024) and six hours (Dong  
 258 et al., 2024a), both of which are commonly used to divide continuous datasets into individual  
 259 events. In our preliminary analysis, applying a four-hour threshold resulted in 5–8 more annual  
 260 events (warm-season only) than the six-hour threshold over the study period; however, most of  
 261 these additional events corresponded to the falling limbs of hydrographs during larger storms.

262 Therefore, a six-hour inter-event dry period was adopted to divide the continuous data into  
263 individual storm events. To capture delayed flow responses, the corresponding flow data were  
264 extended by an additional six hours, without overlapping with subsequent events (Dong et al.,  
265 2024a). The same performance metrics used for the continuous flow models were applied to  
266 evaluate the performance of the event-based models.

267 To assess the influence of discretization method on the performance of the models across  
268 different rainfall depths and land use characteristics (urban versus peri-urban), a linear fixed-  
269 effects model was applied. This statistical approach evaluates how specific factors affect an  
270 outcome (i.e., response variable; Equation 6) (Fox, 2015).

271  $y_i = \sum \beta_j \cdot x_{i,j} + \alpha_j + \varepsilon_{i,j}$  Equation 6

272 here  $\beta_j$  is a coefficient describing the influence of the  $j$ th predictor  $x_{i,j}$  on performance metric  
273  $y_i$  in the  $i$ th event,  $\alpha_j$  is the unobserved event-invariant effect (e.g., the distinct effects of upper  
274 and lower watershed land uses)  $\varepsilon_{i,j}$  is a stochastic error term with an expected value of zero  
275  $E[\varepsilon_{i,j}] = 0$ , and constant variance  $E[\varepsilon_{i,j}^2] = \sigma^2$ .

276 Model performance metrics, including NSE, peak error, volume error, and time-to-peak error,  
277 were used as response variables ( $y_i$ ). Discretization method, rainfall depth, and watershed land  
278 use characteristics were treated as fixed effects (predictors) to test whether variations in model  
279 performance could be attributed to these factors. Events with rainfall depths less than 1 mm were  
280 excluded to reduce noise from low-intensity events that do not generate runoff. Categorical  
281 predictors were modeled as binary: sewer-based discretization and lower outlet were assigned as  
282 0, while topography-based discretization and upper outlet were assigned as 1.

283 Finally, the hydrological interpretability of parameter values, defined as the extent to which the  
284 calibrated model parameters physically reflect watershed characteristics and can be used to  
285 interpret underlying hydrological processes, was assessed. For this, Spearman's correlation  
286 analysis was used to examine the relationships between discretization-related parameters  
287 (including imperviousness, slope, drainage area, and width) and subcatchment outputs (e.g.,  
288 runoff volume and peak runoff rate) across all subcatchments, with stronger correlations  
289 indicating greater physical relevance.

290 **3. Results and Discussion**

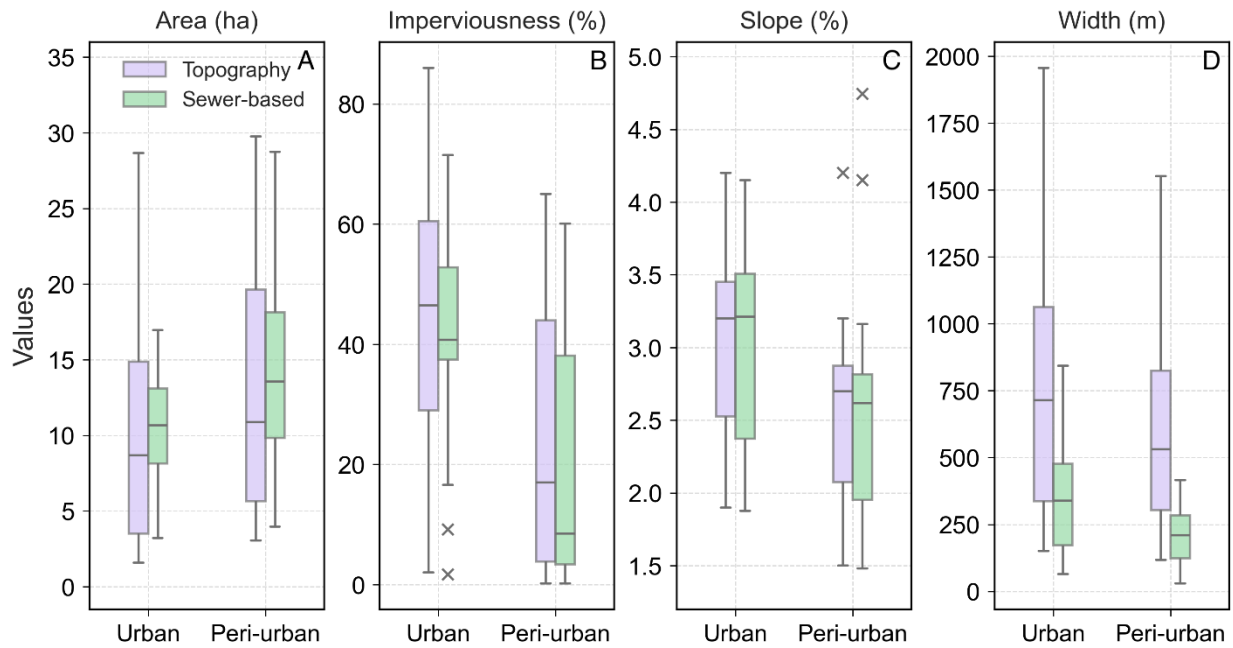
291 **3.1 Model configurations**

292 Model configurations derived from the two discretization approaches are shown in Figure 1B-C.  
293 The sewer geometry-based model comprised 44 subcatchments, with 19 of these subcatchments  
294 located in the upper urban watershed. All subcatchments except two have average elevations  
295 higher than their outlet node elevations (Figure 1C). The two subcatchments with average  
296 elevations slightly lower than those of their corresponding outlet nodes had elevation differences  
297 less than 0.1%. This suggests the “naive” surface-to-node flow assumption (i.e., routing runoff  
298 toward the nearest node) is generally acceptable, as this modest elevation difference could result  
299 from data processing processes or limitations in DEM resolution (Dong et al., 2022). This aligns  
300 with the findings of Dong et al. (2022), who showed that most subcatchments in their modeled  
301 sewershed satisfied the surface-to-node assumption. In comparison to the sewer geometry-based  
302 model, the topography-based model has 52 subcatchments, with 22 located in the upper urban  
303 watershed. Due to incomplete infrastructure documentation in the lower peri-urban watershed,  
304 particularly around a newly developed residential neighborhood (near Location L2 in Figure

305 1A), subcatchment boundaries and flow routing were primarily determined using known major  
306 trunk sewers and input from municipal stormwater engineers. These data limitations may  
307 contribute to uncertainty in parameter estimation and calibration for the lower watershed. Further  
308 details are discussed in the sections below.

309 **3.2 Comparison of discretization-related parameters**

310 A comparison of the discretization-related subcatchment physical parameters between the  
311 topography- and sewer geometry-based models is shown in Figure 2. For both models,  
312 subcatchment areas in the lower peri-urban watershed were generally larger than those in the  
313 upper urban watershed. In the sewer geometry-based model, the area of the subcatchments varies  
314 from 3.1–17.2 ha (mean = 11.6 ha) in the upper urban watershed and from 3.9–28.8 ha (mean  
315 =14.7 ha) in the lower peri-urban watershed, while in the topography-based model, the area  
316 varies from 1.9–28.7 ha (mean = 10.3 ha) in the upper watershed and from 3.1–29.9 ha (mean  
317 =13.4 ha) in the lower watershed. In the sewer geometry-based model, the delineation resolution  
318 (shape) depends on the spatial distribution of nodes (e.g., sewer inlets), resulting in finer  
319 subcatchments in the upper watershed where nodes were more densely distributed. In contrast,  
320 topography-based delineation was determined based on terrain variation and flow paths. In the  
321 upper urban watershed, anthropogenic modifications to the terrain, such as road crowns and lot  
322 grading, could alter natural flow paths, thereby producing relatively smaller drainage areas.



323

324 **Figure 2.** Comparison of discretization-related physical parameters (A) area, (B)  
 325 imperviousness, (C) slope, and (D) width for the subcatchments in the two models. The  
 326 horizontal lines within the boxes show the median value. The bottom and top of the box show the  
 327 25th and 75th quantiles. The whiskers extend 1.5 times the interquartile range (IQR; 25th and  
 328 75th quantiles).

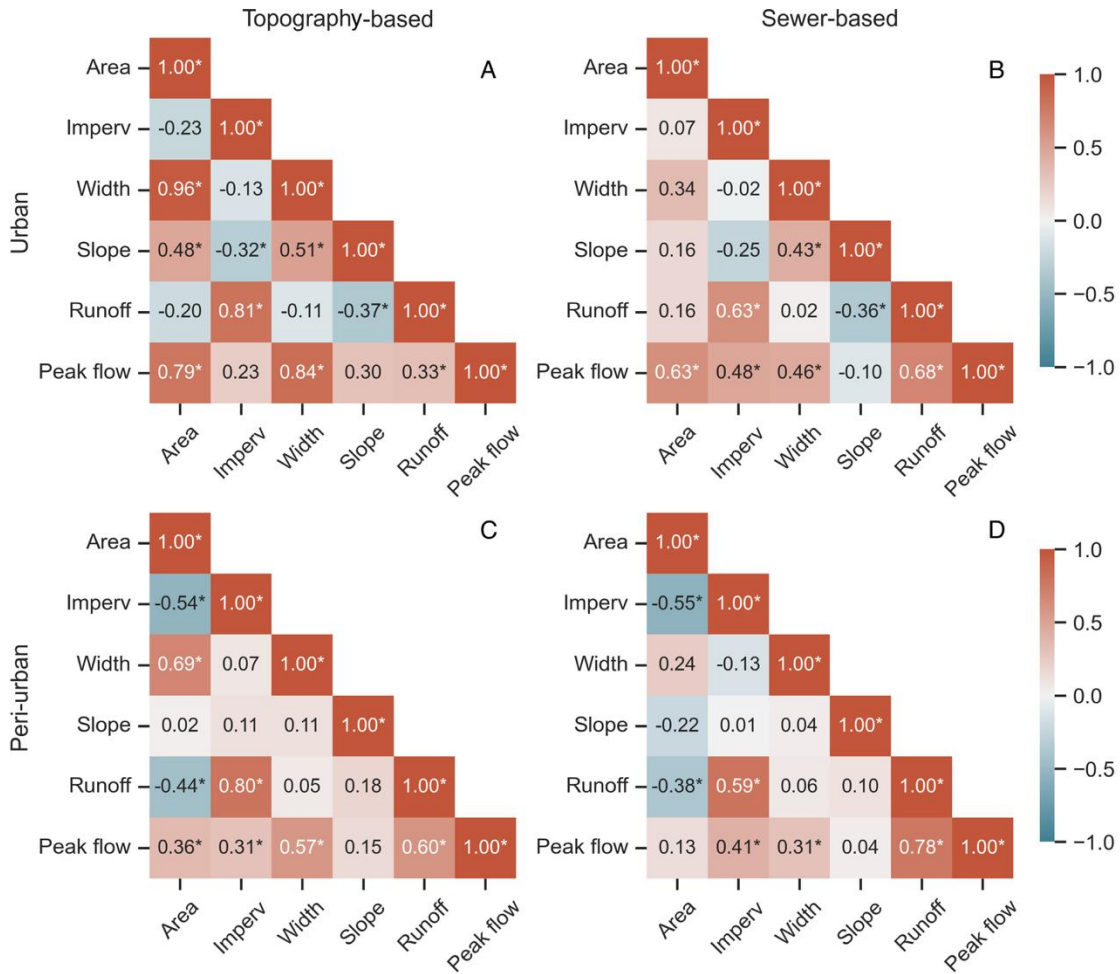
329 In the urban watershed, the subcatchments in the topography-based model had greater variability  
 330 in imperviousness compared to the sewer geometry-based model (Figure 2B). This may be due  
 331 to the drainage areas (i.e., subcatchments) produced by the topography-based delineation  
 332 aggregating less heterogeneous land cover within individual subcatchments. In contrast, the  
 333 sewer geometry-based delineation, which does not account for topography, resulted in  
 334 subcatchments with more mixed land cover (varying degrees of imperviousness), ultimately  
 335 resulting in a narrower range of imperviousness. In the lower peri-urban watershed, the  
 336 imperviousness generated by the two models was comparable, likely due to the lower degree of

337 urbanization in the lower watershed. Subcatchment slopes showed limited difference between the  
338 models, with both having steeper slopes in the upper watershed compared to the lower watershed  
339 (Figure 2C and Figure S2C). However, it should be noted that parameter estimates of  
340 imperviousness and slope derived from area-weighted averaging may mask surface heterogeneity  
341 and reduce the variability in parameter estimates. In areas with limited high-resolution spatial  
342 data, parameter homogeneity assumptions within subcatchments can further weaken the  
343 representation of spatial variability, potentially reducing the physical interpretability of model  
344 parameters and overall model performance.

345 Subcatchment width, after calibration, varied considerably between the two models (Figure 2D).  
346 In general, the width values for subcatchments in the topography-based model were larger  
347 compared to the sewer geometry-based model. This suggests that polygon-based subcatchments  
348 created in the sewer geometry-based model tend to generate narrow overland flow paths (or  
349 channels). Considering that the flow paths derived based on terrain variation in the topography-  
350 based model aligned well with the road distributions (Figure S2A), topography-derived  
351 subcatchment width may better reflect the actual overland flow width.

352 Correlation analysis showed that, in both the upper and lower watersheds, the topography-based  
353 model exhibited stronger relationships between the discretization-related physical parameters  
354 and subcatchment hydrological outputs (i.e., surface runoff volume and peak runoff rate) (Figure  
355 3). While the strength of correlation between subcatchment parameter values and model outputs  
356 does not directly influence model performance, it provides a useful means to assess whether  
357 these parameters physically represent hydrological processes, based on current understanding of  
358 their influence on runoff generation and flow dynamics. Two strong, positive correlations,  
359 reflecting key input-output relationships, have been consistently observed and are well-

360 established: (1) between imperviousness and runoff volume, and (2) between subcatchment  
361 width and peak flow (Behrouz et al., 2020, Dong et al., 2022). If model parameters are better  
362 estimated in one model, we would expect stronger correlation strengths between these two input-  
363 output pairs. Impervious was more strongly correlated with runoff volume in the topography-  
364 based model (mean  $\rho$  across the upper and lower watersheds = 0.81) than in the sewer geometry-  
365 based model (mean  $\rho$  = 0.61) (Figure 3). Similarly, peak flow was more strongly correlated with  
366 subcatchment width in the topography-based model (mean  $\rho$  = 0.71) compared to the sewer  
367 geometry-based model (mean  $\rho$  = 0.39). These results indicate that the parameter values from the  
368 topography-based model may have greater hydrological interpretability. In addition, stronger  
369 inter-parameter correlations were observed in the topography-based model. For instance, in the  
370 upper urban watershed, subcatchment area was highly correlated with width in the topography-  
371 based model ( $\rho$  = 0.96), compared to a weaker correlation in the sewer geometry-based model ( $\rho$   
372 = 0.34). For an ideal discretization, minor changes in drainage area boundaries should not  
373 substantially alter the estimation of actual flow paths (e.g., runoff traveling along roads before  
374 entering a sewer inlet), although changes in the boundaries may influence the volume of runoff  
375 entering the sewer inlet. The stronger correlation strength between subcatchment area and width  
376 observed in the topography-based model suggests that this discretization approach may produce  
377 more consistent estimates of flow path lengths. Overall, the comparison of parameter values and  
378 the results of correlation analysis suggest that the topography-based discretization approach may  
379 yield more physically meaningful parameter values than the sewer geometry-based discretization  
380 approach.



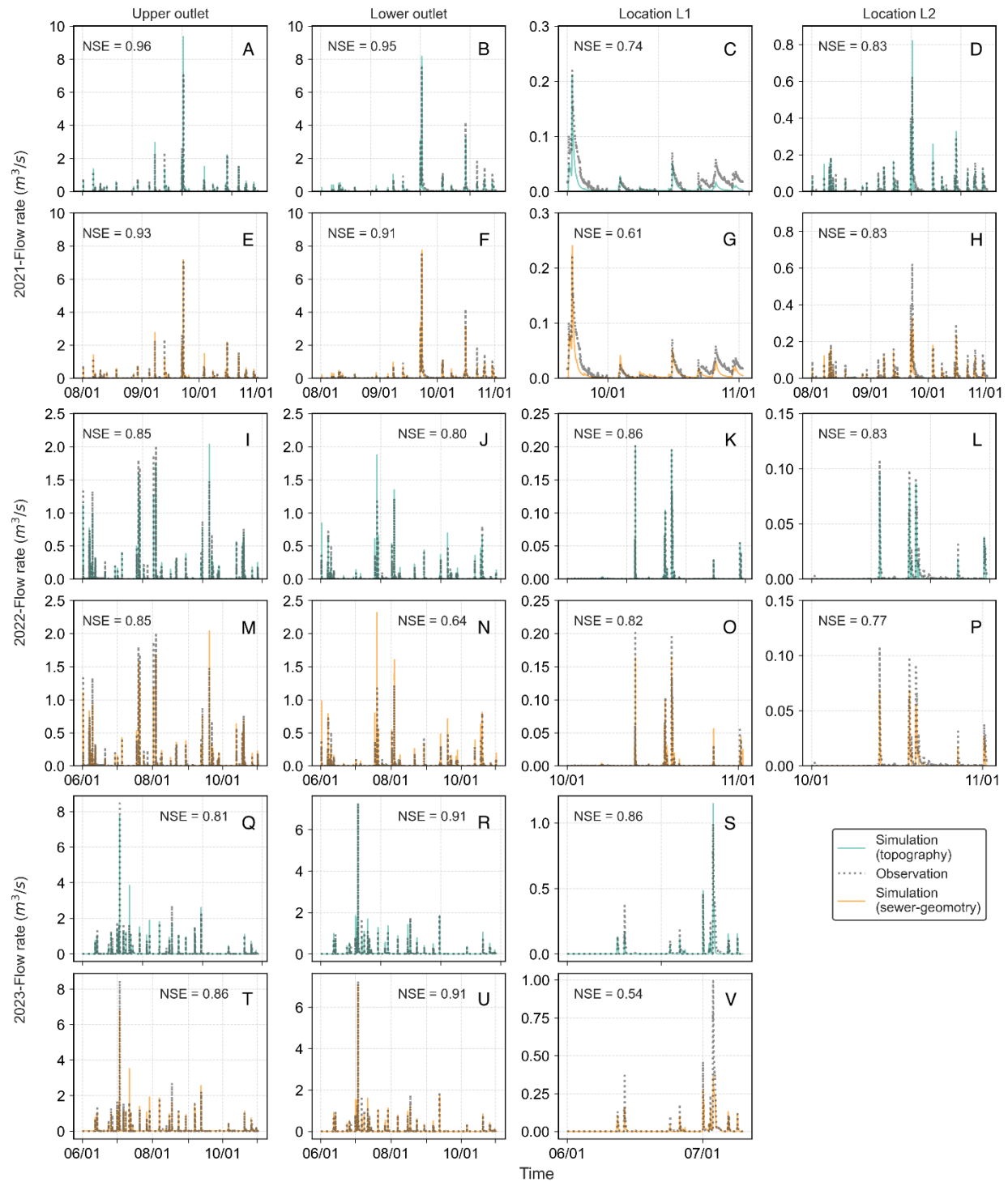
381

382 **Figure 3.** Spearman correlation coefficients across discretization-related subcatchment physical  
 383 parameters (area, width, imperviousness, and slope) and model outcomes (subcatchment runoff  
 384 volume, represented by runoff in the figure, and peak flow): (A) topography-based model for the  
 385 upper urban watershed, (B) sewer geometry-based model for the upper urban watershed, (C)  
 386 topography-based model for the lower peri-urban watershed, and (D) sewer geometry-based  
 387 model for the lower peri-urban watershed. An asterisk (\*) indicates values with  $p < 0.01$ .

388 **3.3 Model performance evaluation**

389 **3.3.1 Overall model performance for continuous simulations**

390 Continuous model calibration and validation results are provided in Figure 4 and Table S3. Both  
391 models achieved high NSE values ( $> 0.9$ ) during calibration using 2021 flow data at the lower  
392 and upper watershed outlets, indicating good agreement between simulated and observed flows.  
393 At the upper outlet, NSE values were 0.96 for the topography-based model and 0.93 for the  
394 sewer geometry-based model. At the lower outlet, NSE values were 0.95 and 0.91, respectively.  
395 Validation using 2022-2023 data suggests slightly reduced model performance for both models,  
396 but the simulated flows still matched well with the observations, with all NSE values  $> 0.8$   
397 except for the sewer geometry-based model at the lower outlet in 2022 (0.64). In addition, at the  
398 upper outlet, the topography-based model produced smaller absolute runoff volume errors (-  
399 6.5% and -13.2% for 2022 and 2023, respectively) and peak flow errors (2.6% and -8.1%)  
400 compared to the sewer geometry-based model, which had volume errors of -28.1% and -22.6%,  
401 and peak flow errors of 2.6% and -19.5% for 2022 and 2023, respectively (Table S3 and Figure  
402 S3). Similar differences in runoff volume and peak flow errors between the models were  
403 observed at the lower outlet, except in 2023, when the absolute runoff volume error for the  
404 topography-based model (25.1%) was higher than that of the sewer geometry-based model (-  
405 8.1%).

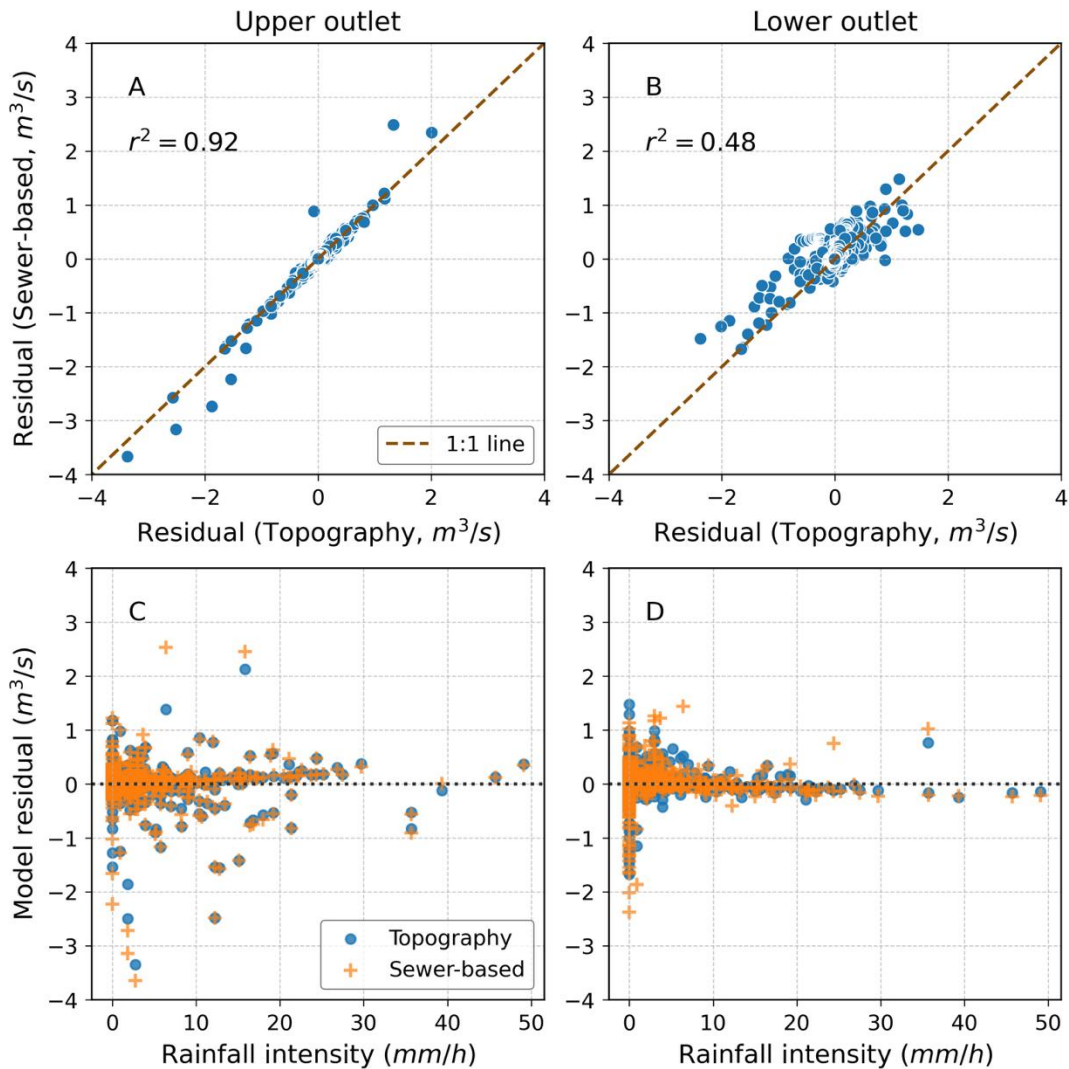


406

407 **Figure 4.** Simulation results at the upper and lower outlets and at the two flow monitoring  
 408 locations within the upper (L1) and lower (L2) watersheds. Data from 2021 at the two outlets

409 were used for model calibration (A–H), while the remaining data were used for model validation  
410 (I–P for 2022 and Q–V for 2023).

411 Flow residuals at the upper outlet from the two models were similar and tightly clustered around  
412 the 1:1 line ( $R^2 = 0.92$ , Figure 5A). These results suggest that the discretization approach used  
413 had limited influence on error structure at the outlet of the urban watershed. In contrast, residuals  
414 between the two models diverged substantially at the lower outlet ( $R^2 = 0.48$ , Figure 5B). This  
415 indicates increased sensitivity to discretization approach used in peri-urban areas. In addition, for  
416 both models, residuals decreased as rainfall intensity increased (Figure 5C–D). This may be  
417 because infiltration, evapotranspiration, and groundwater processes become more important for  
418 smaller rainfall events particularly in the peri-urban area and it is possible that these processes  
419 may be less accurately represented (Dong et al., 2024b, Irvine et al., 2024, Vrugt et al., 2024).  
420 The lower model performance for the 2022 validation period could therefore be due to the  
421 relatively dry weather and the resulting low-flow conditions during that year. These findings  
422 indicate that the faster, simpler sewer geometry-based discretization approach may be sufficient  
423 for simulating outlet flows in urban watersheds. However, in peri-urban areas with more  
424 complex, terrain-driven runoff pathways, even though both models were able to capture the  
425 observed overall flow processes at the lower outlet, the topography-based model generally  
426 performed better than the sewer geometry-based model, as indicated by its relatively higher NSE  
427 values.



428

429 **Figure 5.** Comparisons of flow residuals (difference between simulated and observed flows)  
 430 between the topography- and sewer geometry-based model at the (A) upper outlet and (B) lower  
 431 outlet, and relationships between residuals and rainfall intensity at the (C) upper outlet and (D)  
 432 lower outlet.

433 At the two monitoring sites located within the upper and lower watersheds (L1 and L2), although  
 434 both models showed decreased performance compared to simulating flows at the watershed  
 435 outlets, simulated flows from the topography-based model showed stronger agreement with

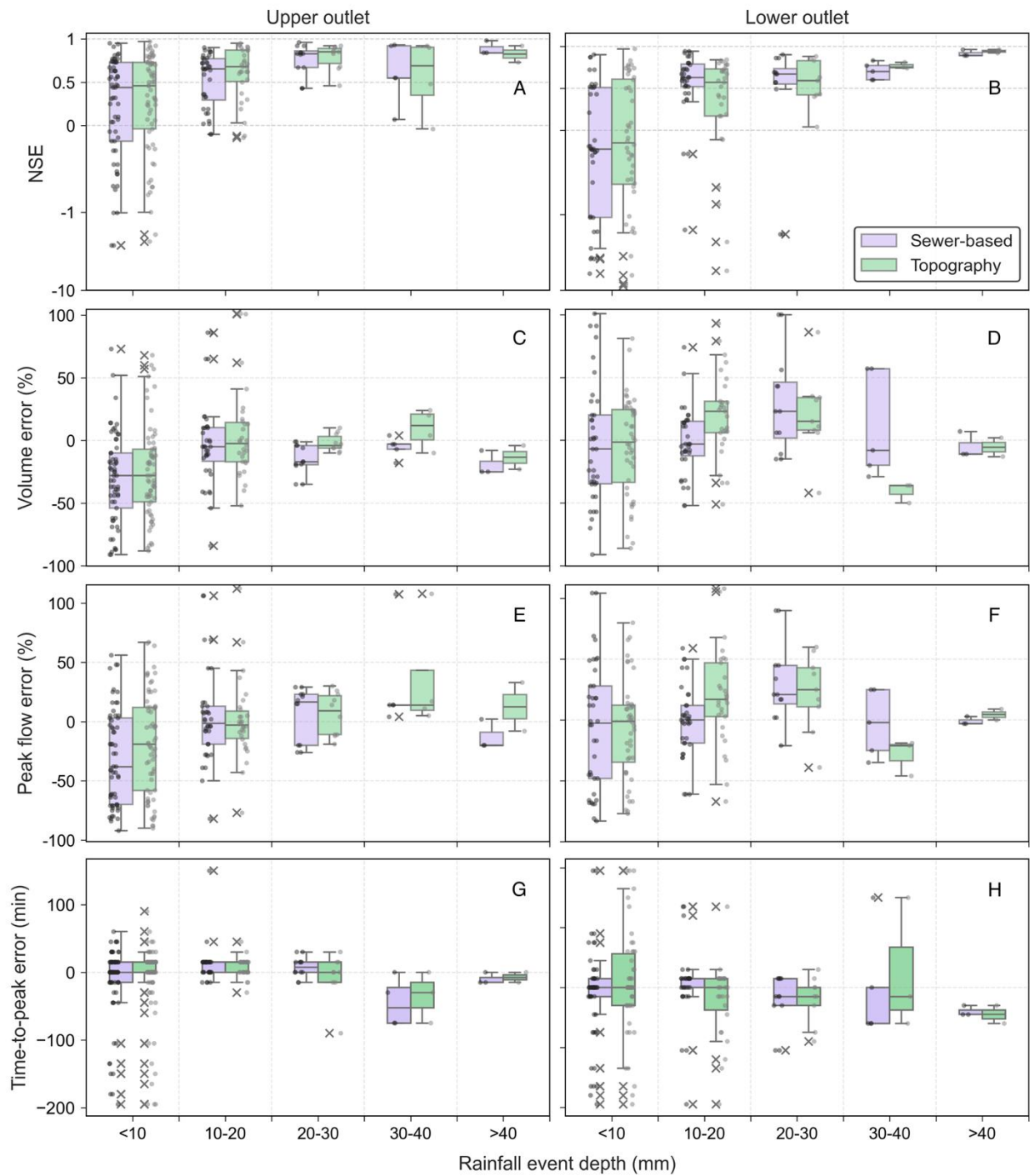
436 observed flows compared with the sewer geometry-based model (Figure 4 and Table S3). The  
437 mean NSE values during the validation period were 0.82 and 0.83 at L1 and L2, respectively, for  
438 the topography-based model compared with 0.66 at L1 and 0.80 at L2, respectively, for the  
439 sewer-based model. At location L1, within the upper urban watershed, the lower performance of  
440 the sewer geometry-based model may be due to the less representative subcatchment boundaries  
441 generated using Thiessen polygons, as discussed in Section 3.2. In contrast, both models yielded  
442 similar NSE values at location L2, within the peri-urban area, where the relatively flat terrain and  
443 sparsely distributed drainage infrastructure potentially reduced differences caused by the varying  
444 drainage boundaries between the two models. However, when comparing runoff volume and  
445 peak flow errors (Table S3), the topography-based model still outperformed the sewer geometry-  
446 based model at location L2. Overall, these results indicate that while both models can effectively  
447 replicate observed flows at the outlets of urban and peri-urban watersheds (with comparable NSE  
448 values), the topography-based model was more consistent in simulating observed flows at the  
449 monitoring sites located within the watershed. Therefore, to further compare model performance  
450 in simulating outlet flows, the next section focuses on evaluating event-based model  
451 performance at watershed outlets.

### 452 **3.3.2 Model performance across individual events**

453 The total number of individual events ranged from 36 to 42, with a mean of 39 events over the  
454 simulation period (2021-2023). Model performance was evaluated at the event scale to examine  
455 the influence of rainfall characteristics on simulation accuracy (Figure 6). In general, better  
456 model performance was observed during larger rainfall events for the two models. At the upper  
457 outlet, the mean NSE values increased from 0.24 to 0.83 for the topography-based model and  
458 from 0.17 to 0.89 for the sewer geometry-based model as event depth increased from <10 mm

459 to >40 mm. Correspondingly, the absolute mean runoff volume error decreased from 25% to  
460 13% for the topography-based model and from 30% to 19% for the sewer geometry-based  
461 model. Further, the absolute mean peak flow error was reduced from 18% to 12% and from 30%  
462 to 12%, respectively, as the event depth increased from <10 mm to >40 mm. Although the  
463 reduction in mean time-to-peak errors was relatively small (~15 min) for both models as rainfall  
464 depth increased from <10 mm to >40 mm, the range of these errors decreased by more than  
465 fivefold. Similar trends in the performance metrics were observed for the lower outlet; however,  
466 the performance metrics exhibited greater variability at the lower outlet compared to the upper  
467 outlet, suggesting that accurately simulating stormwater flow in peri-urban areas, where natural  
468 and urban hydrological processes occur concurrently, is more challenging than in highly  
469 urbanized areas.

470 Overall, consistent trends in performance metrics across storm magnitudes and between the two  
471 models suggest that model performance was sensitive to event rainfall depth. Smaller storms  
472 (<10 mm) exhibited greater variability and lower accuracy, likely because the simplified  
473 formulations of infiltration and evaporation (e.g., the assumption of soil saturation in the Green-  
474 Ampt infiltration equation) may not fully represent the spatial and temporal heterogeneity of  
475 initial soil moisture conditions across subcatchments. Consequently, greater attention may be  
476 needed to improve the parameterization of these hydrological processes beyond the selection of  
477 an appropriate discretization method. It is possible that the observed influence of rainfall depth  
478 on model performance may be biased by the uneven distribution of events across rainfall  
479 categories (e.g., 61 events with rainfall depth <10 mm compared with 9 events with depth >30  
480 mm). A more robust evaluation of model performance requires additional rainfall-runoff data to  
481 enable more balanced comparisons among rainfall depth categories.



482

483 **Figure 6.** Comparison of (A-B) NSE values, (C-D) runoff volume errors (%), (E-F) peak flow  
 484 errors (%), and (G-H) time-to-peak error (min) between the topography-based and sewer-based  
 485 models for individual events. Comparison between events is presented in five event depth

486 classes: < 10mm, 10-20mm, 20-30mm, 30-40mm, and >40mm. Gray dots indicate the  
487 performance of individual events. For readability, NSE values between -1 and 1 are presented on  
488 a linear scale, while values outside this range are shown on a log scale.

489 The effects of rainfall depth, discretization approach, and watershed land use characteristics on  
490 model performance were further assessed using a linear fixed-effects model (Table 1). Results  
491 show the linear fixed-effects model significantly explained the variance in NSE, peak error, and  
492 volume error (all  $p < 0.001$ ; Table S4), whereas it did not significantly explain the variance in  
493 time-to-peak error ( $p = 0.21$ ). Across all performance metrics evaluated, land use characteristics  
494 were a statistically significant predictor of model performance. Note that the lower watershed  
495 outlet and sewer geometry-based model were designated as the control group (zero values), so  
496 the regression coefficients provided in Table 1 represent differences relative to this baseline.

497 Model performance at the upper urban watershed outlet was significantly better than at the lower  
498 outlet, with mean runoff volume and peak flow errors 0.1 and 0.2 lower, respectively, and a  
499 mean NSE value that was 0.5 higher (Table 1). Rainfall depth was also a strong predictor. For  
500 every additional 1 mm of rainfall, the model indicates that the NSE value is expected to increase  
501 by 0.02 with all other variables constant. Similar improvements with increasing rainfall depth  
502 were observed in volume error (0.4% lower for additional 1 mm of rainfall) and peak error (0.7%  
503 lower). However, discretization approach had no significant effect on any performance metric  
504 despite the topography-based model showing slightly better performance (e.g., higher NSE  
505 values) compared to the sewer geometry-based model at the upper outlet in the continuous  
506 simulations (Figure 4). These results suggest that performance of the model at watershed outlets  
507 is most influenced by land use characteristics (urban or peri-urban) and rainfall depth, with  
508 limited sensitivity to the watershed discretization approach used. In other words, for outlet flow

509 simulations, the influence of spatial discretization could be mitigated through model calibration  
510 to achieve an overall water balance across the entire watershed. This was demonstrated in  
511 Section 3.2, where the sewer-geometry-based model exhibited weaker relationships between  
512 parameters and hydrological outputs, yet was able to replicate the observed outlet flows.  
513 Consequently, the effects of spatial discretization are more apparent in simulating flows within  
514 the watershed (as shown in Figure 4 and Table S3). That said, despite its reduced accuracy in  
515 locations within the watershed, the sewer geometry-based model still generated acceptable  
516 results (all NSE values  $> 0.5$ ). Overall, linear fixed-effects model further indicates that simpler  
517 delineation methods, such as the sewer geometry-based approach, may be an acceptable way to  
518 reduce model complexity without significantly compromising simulation accuracy at the outlet.

519 **Table 1.** Results of the fixed effects model for the four performance metrics (NSE, peak flow  
520 error, volume error, and time-to-peak error). The model includes rainfall depth, discretization  
521 approach, and watershed land use characteristics as possible explanatory variables. Values are  
522 reported as estimated coefficients when the p-value is  $<0.05$ . A sign of “-” indicates a coefficient  
523 is not statistically significant ( $p> 0.05$ ), and thus is not reported.

	NSE	Peak flow error	Time-to-peak error	Volume error
Intercept	-0.3	-0.1	-20.8	-
Land use characteristics	0.5	-0.1	21.7	-0.2
Discretization approach	-	-	-	-
Rainfall depth	0.02	0.007	-	0.004

524 **3.4 Implication and trade-offs**

525 Our findings are consistent with previous studies reporting that the two discretization approaches  
526 can yield comparable watershed-scale water balance estimates in urban areas (i.e., at the outlet),

527 such as similar peak flow predictions (Dong et al., 2022). However, our results extend this  
528 understanding by showing that the similarity in water balance estimates tends to decrease,  
529 although not significantly, in peri-urban watersheds, where the topography-based approach is  
530 able to better represent actual flow pathways and drainage boundaries, thereby enhancing flow  
531 simulations within the watershed. This finding suggests that the topography-based approach may  
532 be more appropriate to use across watersheds with varying land-use characteristics. Nevertheless,  
533 previous studies have noted that DEM resolution can substantially influence subcatchment  
534 delineation outcomes and model performance (Zhou et al., 2021, Sokolovskaya et al., 2023), and  
535 that high-resolution DEMs are not uniformly available across urban areas (Hawker et al., 2019).  
536 Therefore, the choice of discretization strategy should consider the spatial data availability,  
537 modeling objectives, and land use and drainage characteristics of the watershed.

538 Key considerations distinguishing the two approaches are outlined in Table 2. The topography-  
539 based model showed a strong relationship between physical parameters and hydrological  
540 responses, making it suitable for simulating flow processes within the watershed and assessing  
541 the impacts of land use changes or stormwater management scenarios (e.g., green infrastructure  
542 placement), when high-resolution spatial data are available. In contrast, the simplicity and  
543 efficiency of the sewer geometry-based discretization approach make it suitable for fast, large-  
544 scale applications, particularly when sewer datasets are the primary spatial input and the model  
545 objective is on sewer hydraulics at the outlet, such as simulating combined sewer overflows  
546 (CSOs). However, this simplicity comes at the cost of reduced hydrological interpretability of  
547 parameter values and a lower capability to simulate flows at locations within the watershed. A  
548 hybrid discretization approach may also be applied by integrating topography-based surface  
549 delineation with geometry-based drainage representation. This approach can be useful in data-

550 limited areas, where low-resolution or incomplete spatial data could introduce substantial  
 551 uncertainty in defining flow pathways and drainage boundaries. In such cases, hybrid  
 552 discretization provides means to adjust model configurations to balance the influence of  
 553 topographic conditions and sewer infrastructure distributions on flow routing, thereby supporting  
 554 exploratory and preliminary analyses for design and planning purposes.

555 **Table 2.** Key differences between topography-based and sewer geometry-based discretization  
 556 approaches.

Aspect	Topography-Based Approach	Sewer Geometry-Based Approach
Stormwater flow prediction at the outlet	High accuracy	Moderate to high accuracy
Simulation of flows within watershed	High accuracy	Adequate overall but less accurate for peak flow
Hydrological representation	Strong correlation between physical parameters and hydrological processes	Relatively weak correlation
Drainage characteristics	Preserves terrain-driven overland flow paths	Tends to generate long, narrow overland flow paths
Rainfall depth impact	High impact on performance	High impact on performance
Implementation complexity	Requiring high resolution DEM, spatial processing, and expert judgment	Low DEM data requirement and single Thiessen polygon generation
Watershed suitability	Both urban and peri-urban watersheds	Better for urban watersheds
Case suitability	Preferred when surface heterogeneity is an important consideration. Better for scenarios of land use, GI design, flooding detection	Effective when primarily interested in outlet flow responses, suitable for fast drainage planning and scenario testing in areas with reliable sewer data but limited high-resolution DEMs

557 Finally, it is important to note that while the findings of this study should be transferable for  
 558 moderately sized mixed watersheds, uncertainties in drainage boundary delineation and  
 559 parameter estimation may propagate and accumulate through flow routing from smaller to larger

560 scales. That is, when these approaches are applied to larger or more complex systems, the  
561 influence of subcatchment delineation on watershed-scale water balance estimates may become  
562 more pronounced. Therefore, future research should further assess the scalability of these  
563 discretization approaches in larger and more heterogeneous watershed settings.

564 **4. Conclusion**

565 This study evaluated the influence of topography-based and sewer geometry-based discretization  
566 strategies on stormwater flow simulations across spatial scales, as well as their effects on model  
567 hydrological representation and parameter interpretation in a mixed urban and peri-urban  
568 watershed. Simulation results showed that both models were capable of reproducing observed  
569 watershed outlet flows (e.g., mean NSE values of 0.88 and 0.85 for the topography-based and  
570 sewer geometry-based models, respectively). However, topography-based discretization  
571 produced parameter values with greater hydrological interpretability and yielded more consistent  
572 model performance in simulating flows at monitoring sites located within the watershed, with  
573 NSE values ranging from 0.74–0.86 compared to 0.55–0.83 for the geometry-based model. It is  
574 important to note that discretization outcomes from the topography-based approach can be  
575 affected by DEM resolution, which will in turn influence parameter estimation and model  
576 performance. As a result, in data-limited areas where high-resolution DEMs are unavailable, the  
577 sewer geometry-based approach can provide a simplified, yet efficient and practical, alternative  
578 for watershed discretization, particularly when the simulation objective is on outlet flows.  
579 It is expected that when these approaches are applied to larger or more complex systems,  
580 uncertainties in drainage boundary delineation may propagate from smaller to larger scales,  
581 leading to more pronounced effects on watershed-scale water balance. Therefore, future work is

582 needed to evaluate how parameter estimates and model performance vary in larger and more  
583 complex watershed settings, and to assess how spatial scale influences model calibration and  
584 validation under different rainfall and land-use conditions. Overall, this study highlights the  
585 significant influence of discretization strategy choice on model robustness across spatial scales  
586 and provides practical guidance for urban stormwater modelers and planners in selecting an  
587 appropriate modeling approach based on watershed land-use characteristics and data availability.

588 **Acknowledgement**

589 This work was supported by Ontario Ministry of the Environment, Conservation, and Parks  
590 (MECP; Grant number- COA-2021-01-1-1556939549), and NSERC Alliance Program (Grant  
591 number: ALLRP: 585967-23). We also thank Dillon Vyn who completed the fieldwork for flow  
592 data collection. We thank the City of London (Adrienne Sones, Shawna Chambers) and UTRCA  
593 (Imtiaz Shah) for their contribution to this project.

594 **References**

595 Alivio, M.B., Radinja, M., Šraj, M., Gribovszki, Z., Bezak, N., 2024. Comparative analysis of  
596 event runoff coefficients and curve numbers in contrasting urban environments based on  
597 observed rainfall-runoff data. *J. Hydrol.* 645, 132135.  
598 <https://doi.org/10.1016/j.jhydrol.2024.132135>

599 Behrouz, M.S., Zhu, Z., Matott, L.S., Rabideau, A.J., 2020. A new tool for automatic calibration  
600 of the Storm Water Management Model (SWMM). *J. Hydrol.* 581, 124436.  
601 <https://doi.org/10.1016/j.jhydrol.2019.124436>

602 Bibi, T.S., 2022. Modeling urban stormwater management in the town of Dodola based on  
603 landuse and climate change using SWMM 5.1. *J. Hydrol. Reg. Stud.* 44, 101267.  
604 <https://doi.org/10.1016/j.ejrh.2022.101267>

605 Bisht, D.S., Chatterjee, C., Kalakoti, S., Upadhyay, P., Sahoo, M., Panda, A., 2016. Modeling  
606 urban floods and drainage using SWMM and MIKE URBAN: a case study. *Nat. Hazards*  
607 84, 749–776. <https://doi.org/10.1007/s11069-016-2455-1>

608 Braud, I., Fletcher, T.D., Andrieu, H., 2013. Hydrology of peri-urban catchments: Processes and  
609 modelling. *J. Hydrol.* 485, 1–4. <https://doi.org/10.1016/j.jhydrol.2013.02.045>

610 Broekhuizen, I., Leonhardt, G., Marsalek, J., Viklander, M., 2020. Event selection and two-stage  
611 approach for calibrating models of green urban drainage systems. *Hydrol. Earth Syst. Sci.*  
612 24, 869–885. <https://doi.org/10.5194/hess-24-869-2020>

613 Dobson, B., Watson-Hill, H., Muhandes, S., Borup, M., Mijic, A., 2022. A Reduced Complexity  
614 Model With Graph Partitioning for Rapid Hydraulic Assessment of Sewer Networks.  
615 *Water Resour. Res.* 58, e2021WR030778. <https://doi.org/10.1029/2021WR030778>

616 Dong, Z., Bain, D.J., Akcakaya, M., Ng, C.A., 2022. Evaluating the Thiessen polygon approach  
617 for efficient parameterization of urban stormwater models. *Environ. Sci. Pollut. Res.* 30,  
618 30295–30307. <https://doi.org/10.1007/s11356-022-24162-7>

619 Dong, Z., Bain, D.J., Buck, J.K., Ng, C., 2024a. Assessment of the long-term hydrological  
620 performance of a green roof system in stormwater control. *J. Environ. Manage.* 370,  
621 122831. <https://doi.org/10.1016/j.jenvman.2024.122831>

622 Dong, Z., Bain, D.J., Paudel, S., Buck, J.K., Ng, C., 2024b. Impact of native vegetation and soil  
623 moisture dynamics on evapotranspiration in green roof systems. *Sci. Total Environ.* 952,  
624 175747. <https://doi.org/10.1016/j.scitotenv.2024.175747>

625 Environment and Climate Change Canada (EMCC), 2024. Historical Temperature Data.  
626 [https://climate.weather.gc.ca/historical\\_data/search\\_historic\\_data\\_e.html](https://climate.weather.gc.ca/historical_data/search_historic_data_e.html)

627 Fox, J., 2015. Applied regression analysis and generalized linear models. Sage publications.

628 Gironás, J., Niemann, J.D., Roesner, L.A., Rodriguez, F., Andrieu, H., 2010. Evaluation of  
629 Methods for Representing Urban Terrain in Storm-Water Modeling. *J. Hydrol. Eng.* 15,  
630 1–14. [https://doi.org/10.1061/\(ASCE\)HE.1943-5584.0000142](https://doi.org/10.1061/(ASCE)HE.1943-5584.0000142)

631 Hawker, L., Neal, J., Bates, P., 2019. Accuracy assessment of the TanDEM-X 90 Digital  
632 Elevation Model for selected floodplain sites. *Remote Sens. Environ.* 232, 111319.  
633 <https://doi.org/10.1016/j.rse.2019.111319>

634 Hopkins, K.G., Bain, D.J., Copeland, E.M., 2014. Reconstruction of a century of landscape  
635 modification and hydrologic change in a small urban watershed in Pittsburgh, PA.  
636 *Landsc. Ecol.* 29, 413–424. <https://doi.org/10.1007/s10980-013-9972-z>

637 Irvine, D.J., Singha, K., Kurylyk, B.L., Briggs, M.A., Sebastian, Y., Tait, D.R., Helton, A.M.,  
638 2024. Groundwater-Surface water interactions research: Past trends and future directions.  
639 *J. Hydrol.* 644, 132061. <https://doi.org/10.1016/j.jhydrol.2024.132061>

640 Javan, K., Banihasemi, S., Nazari, A., Roozbahani, A., Darestani, M., Hossieni, H., 2025.  
641 Coupled SWMM-MOEA/D for multi-objective optimization of low impact development  
642 in urban stormwater systems. *J. Hydrol.* 656, 133044.  
643 <https://doi.org/10.1016/j.jhydrol.2025.133044>

644 Jefferson, A.J., Bhaskar, A.S., Hopkins, K.G., Fanelli, R., Avellaneda, P.M., McMillan, S.K.,  
645 2017. Stormwater management network effectiveness and implications for urban  
646 watershed function: A critical review. *Hydrol. Process.* 31, 4056–4080.  
647 <https://doi.org/10.1002/hyp.11347>

648 Jivani, S., 2024. Modelling seasonal non-point source phosphorus loads from a mixed urban and  
649 agricultural land use watershed.

650 Khatooni, K., Hooshyaripor, F., MalekMohammadi, B., Noori, R., 2025. A new approach for  
651 urban flood risk assessment using coupled SWMM–HEC-RAS-2D model. *J. Environ.*  
652 *Manage.* 374, 123849. <https://doi.org/10.1016/j.jenvman.2024.123849>

653 Krebs, G., Kokkonen, T., Valtanen, M., Setälä, H., Koivusalo, H., 2014. Spatial resolution  
654 considerations for urban hydrological modelling. *J. Hydrol.* 512, 482–497.  
655 <https://doi.org/10.1016/j.jhydrol.2014.03.013>

656 Lee, J.G., Nietch, C.T., Panguluri, S., 2018. Drainage area characterization for evaluating green  
657 infrastructure using the Storm Water Management Model. *Hydrol. Earth Syst. Sci.* 22,  
658 2615–2635. <https://doi.org/10.5194/hess-22-2615-2018>

659 Leitão, J.P., Boonya-aroonnet, S., Prodanović, D., Maksimović, Č., 2009. The influence of  
660 digital elevation model resolution on overland flow networks for modelling urban pluvial  
661 flooding. *Water Sci. Technol.* 60, 3137–3149. <https://doi.org/10.2166/wst.2009.754>

662 Li, J., Huang, G., Chen, W., 2024. Improvement of City Rainfall Model Subcatchment Structure  
663 Based on Urban Hydrology Process. *J. Hydrol. Eng.* 29, 05024001.  
664 <https://doi.org/10.1061/JHYEFF.HEENG-6084>

665 Macro, K., Matott, L.S., Rabideau, A., Ghodsi, S.H., Zhu, Z., 2019. OSTRICH-SWMM: A new  
666 multi-objective optimization tool for green infrastructure planning with SWMM.  
667 *Environ. Model. Softw.* 113, 42–47. <https://doi.org/10.1016/j.envsoft.2018.12.004>

668 Nash, J.E., Sutcliffe, J.V., 1970. River flow forecasting through conceptual models part I — A  
669 discussion of principles. *J. Hydrol.* 10, 282–290. [https://doi.org/10.1016/0022-1694\(70\)90255-6](https://doi.org/10.1016/0022-1694(70)90255-6)

670 Ni, T., Zhang, X., Leng, P., Pelling, M., Xu, J., 2025. Comprehensive benefits evaluation of low  
671 impact development using scenario analysis and fuzzy decision approach. *Sci. Rep.* 15,  
672 2227. <https://doi.org/10.1038/s41598-025-85763-z>

673 Niazi, M., Nietch, C., Maghrebi, M., Jackson, N., Bennett, B.R., Tryby, M., Massoudieh, A.,  
674 2017. Storm Water Management Model: Performance Review and Gap Analysis. *J.*  
675 *Sustain. Water Built Environ.* 3, 04017002. <https://doi.org/10.1061/JSWBAY.0000817>

676 Ontario Ministry of Natural Resources and Forestry (OMNRF), 2019. Authoritative Geospatial  
677 Data. <https://geohub.lio.gov.on.ca/>

678 Perin, R., Trigatti, M., Nicolini, M., Campolo, M., Goi, D., 2020. Automated calibration of the  
679 EPA-SWMM model for a small suburban catchment using PEST: a case study. *Environ.*  
680 *Monit. Assess.* 192, 374. <https://doi.org/10.1007/s10661-020-08338-7>

681 Qi, M., Lehmann, A., Huang, H., Liu, L., Chen, X., 2025. A SWMM-based evaluation of the  
682 impacts of LID and detention basin retrofits on urban flooding. *Urban Water J.* 22, 51–  
683 65. <https://doi.org/10.1080/1573062X.2024.2426590>

684 Rossman, L.A., Huber, W.C., 2016. Storm Water Management Model Reference Manual  
685 Volume I – Hydrology. Washington, DC.

686 Salvadore, E., Bronders, J., Batelaan, O., 2015. Hydrological modelling of urbanized  
687 catchments: A review and future directions. *J. Hydrol.* 529, 62–81.  
688 <https://doi.org/10.1016/j.jhydrol.2015.06.028>

689 Si, Q., Brito, H.C., Alves, P.B.R., Pavao-Zuckerman, M.A., Rufino, I.A.A., Hendricks, M.D.,  
690 2024. GIS-based spatial approaches to refining urban catchment delineation that integrate  
691 stormwater network infrastructure. *Discov. Water* 4, 24. <https://doi.org/10.1007/s43832-024-00083-z>

692 Sokolovskaya, N., Vaughn, C., Jahangiri, H., Smith, V., Wadzuk, B., Ebrahimian, A., Nyquist,  
693 J., 2023. Variability of urban drainage area delineation and runoff calculation with  
694 topographic resolution and rainfall volume. *Water Sci. Technol.* 87, 1349–1366.  
695 <https://doi.org/10.2166/wst.2023.072>

696 Swathi, V., Srinivasa Raju, K., Varma, M.R.R., Sai Veena, S., 2019. Automatic calibration of  
697 SWMM using NSGA-III and the effects of delineation scale on an urban catchment. *J.*  
698 *Hydroinformatics* 21, 781–797. <https://doi.org/10.2166/hydro.2019.033>

701 Tamm, O., Kokkonen, T., Warsta, L., Dubovik, M., Koivusalo, H., 2023. Modelling urban  
702 stormwater management changes using SWMM and convection-permitting climate  
703 simulations in cold areas. *J. Hydrol.* 622, 129656.  
704 <https://doi.org/10.1016/j.jhydrol.2023.129656>

705 Vrugt, J.A., Hopmans, J.W., Gao, Y., Rahmati, M., Vanderborgh, J., Vereecken, H., 2024. The  
706 time validity of Philip's two-term infiltration equation: An elusive theoretical quantity?  
707 *Vadose Zone J.* 23, e20309. <https://doi.org/10.1002/vzj2.20309>

708 Vyn, D.H., 2023. Effect of land use type and stormwater control measures on non-point source  
709 phosphorus concentrations and loads in a cold climate urban subwatershed. *Western*  
710 *University*, London.

711 Warsta, L., Niemi, T.J., Taka, M., Krebs, G., Haahti, K., Koivusalo, H., Kokkonen, T., 2017.  
712 Development and application of an automated subcatchment generator for SWMM using  
713 open data. *Urban Water J.* 14, 954–963. <https://doi.org/10.1080/1573062X.2017.1325496>

714 Wu, Y., She, D., Xia, J., Zhang, Y., Zou, L., 2024. Evaluation of the number of events' influence  
715 on model performance and uncertainty in urban data-scarce areas based on behavioral  
716 parameter ranking method. *J. Hydrol.* 636, 131298.  
717 <https://doi.org/10.1016/j.jhydrol.2024.131298>

718 Zhou, Z., Meneses, D.M., Yu, Y., Gong, J., Guo, Q., 2021. Delineation of Small Flat Watershed  
719 with High-Resolution DEM from Terrestrial Laser Scanning. *J. Hydrol. Eng.* 26,  
720 04021021. [https://doi.org/10.1061/\(ASCE\)HE.1943-5584.0002096](https://doi.org/10.1061/(ASCE)HE.1943-5584.0002096)

721 Zhuang, Q., Li, M., Lu, Z., 2023. Assessing runoff control of low impact development in Hong  
722 Kong's dense community with reliable SWMM setup and calibration. *J. Environ.*  
723 *Manage.* 345, 118599. <https://doi.org/10.1016/j.jenvman.2023.118599>

724